Internal Currents in PEMFC during Start-up or Shut-down

G. Maranzana, O. Lottin, C. Moyne, J. Dillet, A. Lamibrac, J. Mainka, S. Didierjean

This document appeared in

Detlef Stolten, Thomas Grube (Eds.):
18th World Hydrogen Energy Conference 2010 - WHEC 2010
Parallel Sessions Book 1: Fuel Cell Basics / Fuel Infrastructures
Proceedings of the WHEC, May 16.-21. 2010, Essen
Schriften des Forschungszentrums Jülich / Energy & Environment, Vol. 78-1
Institute of Energy Research - Fuel Cells (IEF-3)
Forschungszentrum Jülich GmbH, Zentralbibliothek, Verlag, 2010
ISBN: 978-3-89336-651-4

Internal Currents in PEMFC during Start-up or Shut-down

G. Maranzana, O. Lottin, C. Moyne, J. Dillet, A. Lamibrac, J. Mainka, S. Didierjean, LEMTA, Nancy University – CNRS, Nancy, France

Although several working conditions are known to be damaging to Proton Exchange Membrane Fuel cells (PEMFC), their degradation mechanisms are not fully understood yet [1]. For instance, supplying the fuel cell with dry gases can induce a fast degradation of the electrodes [2] but on the other hand, long-time or repeated storage without purging liquid water from the gas channels accelerates the fuel cell aging. Potential cycling [3] or operation under open-circuit conditions [4] are also to be avoided. This paper reports about an experimental and numerical study of the internal currents that occur during fuel cell start-up under open-circuit conditions. Shut-down/start-up cycling results in performance degradation according to Tang et al., Shen et al. and Kim et al. [5-7]. During start-up, hydrogen pushes oxygen, air, or possibly nitrogen that was introduced for purging water toward the outlet so that for a short time depending on various parameters like the flow rate and the channels geometry, a fraction of the anode compartment is filled with hydrogen while the other part is still occupied by the gas initially present. A potential appears at the inlet of the anode but not at the outlet, which generates internal currents under open-circuit conditions. Although these internal currents are scarcely studied, they were modelled by some authors [8-10] and they can be measured using segmented cells [11, 12]. According to Meyer and Darling [9] internal currents can be at the origin of fuel cell performance decay by creating abnormally high potentials at the cathode, causing carbon corrosion. Starting from experimental data measured thanks to a segmented cell, Siroma et al. [11] suggested that the double layer capacitance could play a major role in the origin of reverse currents and high potentials.

1 Experimental Setup

A segmented fuel cell was designed with the objective to reduce as much as possible the high frequency resistance associated with the current collection in order to obtain a good assessment of the magnitude of the internal currents (*figure 1*). Air and hydrogen flow through five *30 cm* parallel straight channels of 0.7×1 mm² in section. On the anode side, the channels are machined in an aluminum plate that is then gold plated. The cathode plate is in polycarbonate (transparent but non conductive) and the channel ribs are made of *15 mm* long, *1 mm* thick gold plated brass strips. They are inserted only between two adjacent channels so that *4×20 = 80* strips were necessary for the five channels. Each strip is electrically isolated from the preceding and following ones (along the *x* axis in *figure 1*) thanks to a small *2.3×1 mm²*, *80 µm* thick Kapton sheet. The main technical difficulty was to obtain a flat contact surface in order to make the contact resistance between the channel ribs and the backing layer as much uniform as possible. This was done by surfacing the channel ribs once they were embedded in the polycarbonate plate. They were then gold plated in a second step. The MEA (*Jonhson-Matthey*) consists of a 30 *µm* thick *Nafion 212* membrane and of catalytic layers with an average Pt loading of 0.4 *mg cm*$^{-2}$ at the anode and cathode.

The active area is $A = 30\ cm^2$. The GDL is a 190 μm thick carbon fibre paper (*Toray TGP-H-060*). The MEA is not segmented. For these experiments, the four adjacent strips are electrically connected outside the cell, which is equivalent to averaging the current intensity along the *y* direction. Thus, twenty wires (one per segment) drive the current towards twenty $5\ m\Omega$ shunt resistors, which voltage drops allow an indirect measurement of the current intensity. Then, all segments are set to the same potential, as shown in the sketch of *figure 2*. The total resistance between the channel ribs and the point where the twenty segments are connected is about $12\ m\Omega$. The resistance between two consecutive brass strips being of $175\ m\Omega$, it is reasonable to assume that most of the current produced in a segment actually flows through the corresponding connecting wire instead of the GDL thickness according the plane direction. Numerical data (local current intensities and voltage) are recorded at a frequency of 200 *Hz* and with a 16 *bit* resolution thanks to a *National Instrument SCXI* multiplexer.

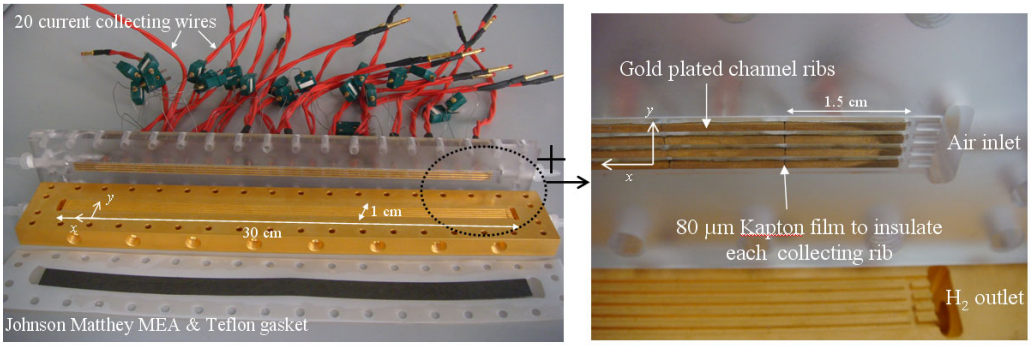

Figure 1: View of the dismantled segmented cell and zoom on the segmented channel ribs.

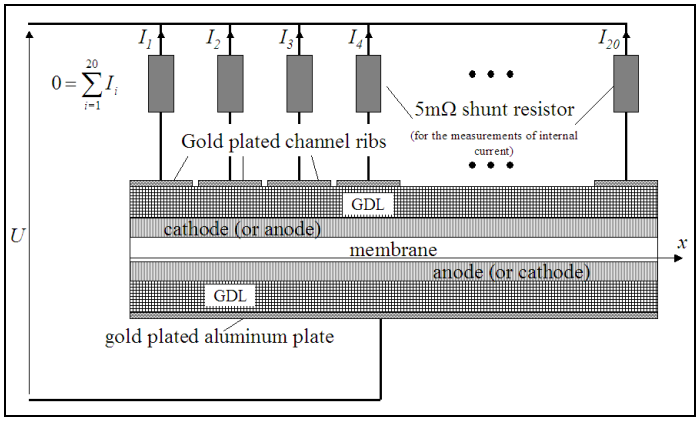

Figure 2: Scheme of the electrical connections.

2 Experimental Results

Several start-up experiments were performed with different values of the hydrogen flow rate, the anode compartment being initially filled with air or nitrogen. Nitrogen was used to study

the effect of a purge after shut-down. The fuel cell was at ambient temperature (22 °C) and air and hydrogen were humidified until saturation using bubblers (also at ambient temperature). The occurrence of internal currents can be seen in *figure 3* with the simultaneous rise of the open circuit potential as functions of time. The hydrogen flow was set to *3 cms*$^{-1}$ and *1 ms*$^{-1}$, which correspond to theoretical values of the current density in steady state of *0.03 Acm*$^{-2}$ and *1 Acm*$^{-2}$ (with a stoichiometry of *1*). The air flow was set to *5 ms*$^{-1}$, which corresponds to a steady state current density of *1 Acm*$^{-2}$ with a stoichiometry of *2*.

The sum of the currents flowing through the twenty segments being null at open circuit, the current that is produced by the first segment is necessarily distributed between the others. Thus, when hydrogen reaches the inlet of the cell the electrical current produced by the first segment flows toward the 19 others so that reverse currents (by reference to the normal fuel cell operation) can be measured. The current produced by the first segment reaches a maximum and then decreases while the hydrogen front is moving forward. Similar current profiles are observed in the other segments but with a lower intensity. Once the hydrogen front has reached the anode outlet, the cell voltage is close to the open circuit voltage and the internal currents have almost entirely disappeared. Their intensity increases with the incoming hydrogen velocity until about *1 ms*$^{-1}$; then, it remains constant whatever the hydrogen velocity, probably because of some imperfections in the experimental setup affecting the time constant of the hydrogen flow. With this fuel cell and in the range of operating conditions we have tested, it can reach a maximum of *1 Acm*$^{-2}$ for positive currents and *0.25 Acm*$^{-2}$ for negative currents.

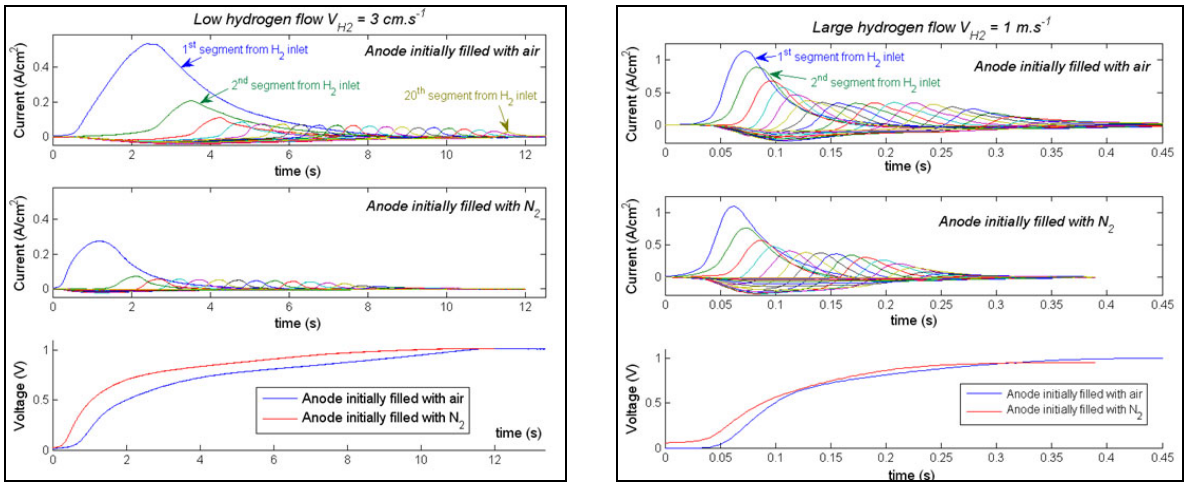

Figure 3: Internal currents and open circuit potential as function of time for two different hydrogen inlet flows and for anode initially filled with air or nitrogen.

The phenomena observed when the gas initially present in the anode compartment is nitrogen or air differ in two points. First, for the lower hydrogen flow rates, the intensity of internal currents is more important with air. The difference is here of the order of 0.2 Acm^{-2}, which cannot be explained by carbon oxidation at the cathode as described in [8-10]: current densities corresponding to carbon oxidation must be of a few mAcm^{-2} [9] only. A more

probable explanation is that the direct oxidation of some hydrogen and oxygen on platinum at the anode improves the hydration of the MEA and raises the local temperature which in turn increases the intensity of internal currents. For the higher hydrogen flow rates, the intensity of internal currents is identical whatever gas is in the anode compartment. This convergence of the magnitude of the internal currents with the hydrogen velocity could be explained either by the imperfections of the experimental setup or by a less significant effect of the MEA hydration mentioned above. The other main difference between air and nitrogen lies in the peak of current density, which happens earlier with nitrogen. Globally, the fuel cell voltage rises also faster with nitrogen. This effect is most probably also linked with the direct oxidation of hydrogen in the presence of oxygen, which slows down the velocity of the hydrogen front in the anode compartment.

3 Modelling

The model presented in the following demonstrates that the occurrence of internal currents can be explained mostly by capacitive effects. Carbon oxidation and other redox mechanisms are considered only via a leakage resistance: redox potentials other than the oxidation of hydrogen are neglected. In order to focus on the main phenomena, the gas initially present in the anode compartment is nitrogen. The case of oxygen is not considered.

For the sake of simplicity, the electrical behaviour of the cell is partially linearized. The basic building block of the model is a generic equivalent circuit of the electrodes which is assumed to be valid whatever the direction of the electrical current (*figure 4*). The electrodes are represented by a double layer capacitance C_{dl} in parallel with a charge transfer resistance R_{tc} and a leakage resistance R_{∞} that accounts for the oxidation of carbon and/or other possible redox phenomena. It is assumed that the value of R_{tc} becomes infinite for negative currents (from anode to cathode) because the voltage maximum value reached during start-up does not allow the electrolysis of water. Moreover, the leakage resistance R_{∞} is neglected when a faradic current exists ($Q_{a,c}>0$): it becomes also infinite. In *figure 4*, the diodes in series with R_{tc} and R_{∞} control their values as functions of the direction of the electrical current. The resistance of the electrolyte and the various contact resistances are accounted for through a single high frequency resistance R_{hf} in series with the anode and the cathode (*figure 5*).

The electrodes as represented in *figure 4* operate following three modes:

- Without hydrogen in the anode compartment, the direction of the electrical current is negative. It flows through the leakage resistance R_{∞} and through the capacitances C_{dlc} and C_{dla} which charge progressively (Q_c, $Q_a < 0$) as the electrical current decreases (in absolute value).
- When hydrogen comes in the anode compartment a voltage E^0 appears between the electrodes and adds to the voltage across to the two partially charged capacitances. The electric current i^k becomes positive and the double layer capacitances C_{dlc} and C_{dla} discharge.
- When the charge of the capacitances becomes null (i.e. when the fuel cell voltage is equal to E^0 or lower) the electrical current i^k becomes a faradic current and it flows through the charge transfer resistances R_{tc} and R_{ta}.

The channel is discretized into *n* segments (*figure 5*) from the inlet (n°*1*) to the outlet (n°*n*). The geometry of the channel and the velocity of hydrogen define a convection time tc_k at which the k^{th} segment is occupied by hydrogen only whereas only nitrogen is present at $t < tc_k$. Air is assumed to be always present in enough quantity in the cathode compartment.

The global equivalent electrical circuit of the fuel cell leads to a system of *3n+1* ordinary differential equations with *3n+1* unknowns. The unknowns are the potential difference between cathode and anode *U*, the current intensity $I^k_{1\le k\le n}$ through the *n* segments, the charge of the *n* cathode capacitances $Q^k_{c\,1\le k\le n}$ and the charge of the *n* anode capacitances $Q^k_{a\,1\le k\le n}$.

$$\begin{cases} U = E^k - R_m I^k - \dfrac{Q_c^k}{C_{dlc}^k} - \dfrac{Q_a^k}{C_{dla}^k} \quad \left(E^k = 0 \text{ if } k > i\right) & 1\le k\le n \\ I^k = \dfrac{dQ_c^k}{dt} + \dfrac{Q_c^k}{R_{tc}^k C_{dlc}^k} = \dfrac{dQ_a^k}{dt} + \dfrac{Q_a^k}{R_{ta}^k C_{dla}^k} \left(R_{ta}^k = R_\infty \text{ if } Q_a^k < 0\right) & 1\le k\le n \\ 0 = \sum_{i=1}^{n} I^i \end{cases}$$

Where E^k stands for the open circuit voltage (in steady state). $E^k = 0\ V$ if $k > i$ and $E^k = E_0$ if $k \le i$. Replacing I^k by its expression (the second equation) in the first and third equations and considering that *U* is constant in all the segments makes it possible to reduce the dimension of the system to 2*n* :

$$\frac{d}{dt}\boldsymbol{Q} = \boldsymbol{M}(t)\boldsymbol{Q} + \boldsymbol{S}(t) \qquad \boldsymbol{Q} = \left(Q_c^1 \cdots Q_c^n \; Q_a^1 \cdots Q_a^n\right)^t$$

Where the remaining unknowns are the charges of the capacitances. $\boldsymbol{M}$ is a $2n\times 2n$ square matrix that is time dependent. The source term $\boldsymbol{S}$ is also time dependent. This system can be easily solved by a Runge-Kutta method but an iterative loop must be used to adjust the location of the hydrogen front by subtracting the consumed quantity - derived from the faradic current - from the total quantity of hydrogen injected. Actually, except in the case of very low hydrogen flowrates, the velocity of the front remains almost constant due to the very low hydrogen consumption. Note that the number of segments used for the simulations (*n = 200*) is much higher than the number of segments in the experimental cell: the numerical results presented below are averaged over *10* consecutive segments. In order to avoid numerical instabilities, it was found convenient to increase linearly E^k with time in the k^{th} segment when $t_{ck} < t < t_{ck+1}$.

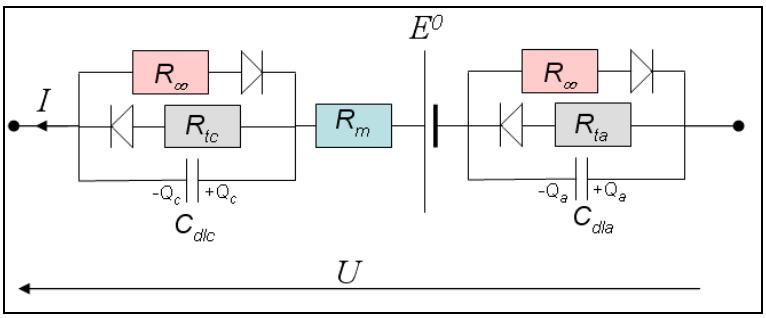

Figure 4: Electrical model of a MEA segment.

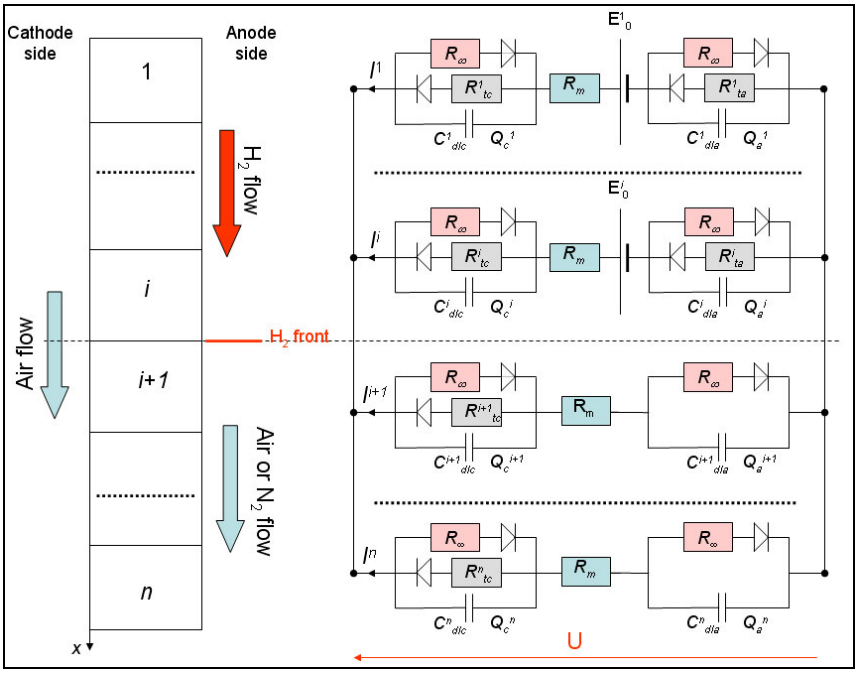

Figure 5: Global equivalent electrical circuit of the fuel cell at time *t* (*t* < t_{ci+1}). The charge transfer resistance R_{tc} at the anode is not represented in the absence of hydrogen because it has no physical meaning.

4 Numerical Results

Figure 6 presents the evolution with time of the internal currents and of the fuel cell voltage as determined by the model with the values of the parameters stated above. The hydrogen flow rate was adjusted so that the inlet velocity corresponds to the experimental values in *figure 3* (*3 cms*$^{-1}$ and *1 ms*$^{-1}$). The experimental (*figure 3*) and numerical results (*figure 6*) are close to each other, at least in qualitative terms. Of course, using constant values for the double layer capacitances, the charge transfer resistances and the leakage resistance is a strong assumption but the model shows that the dominant phenomena are probably linked with the double layer capacitances. Carbon oxidation should occur simultaneously but its contribution to the internal currents is by all appearances negligible.

One can also notice that the model predicts a transient voltage rise over the steady state open circuit voltage ($E_0 = 1\ V$). This voltage rise can be observed experimentally shortly after fuel cell start up: according to these numerical results, it can be explained only by 2D and capacitive effects. However, other phenomena, like hydrogen crossover through the membrane, can show similar effects.

5 Conclusion

Experiments show that the internal currents that occur during PEMFC start-up can reach up to $1\ Acm^{-2}$. This is far more important than the expected order of magnitude of the current densities associated with carbon oxidation, which is only of a few $mAcm^{-2}$. The predominant phenomenon that explains the internal currents is the charge and discharge of the double layer capacitances. A simple model with constant values of the electric parameters yields numerical results close to the experimental ones. It also explains the transient voltage rise (over the steady state open circuit voltage) that is sometimes observed experimentally shortly after the fuel cell start up.

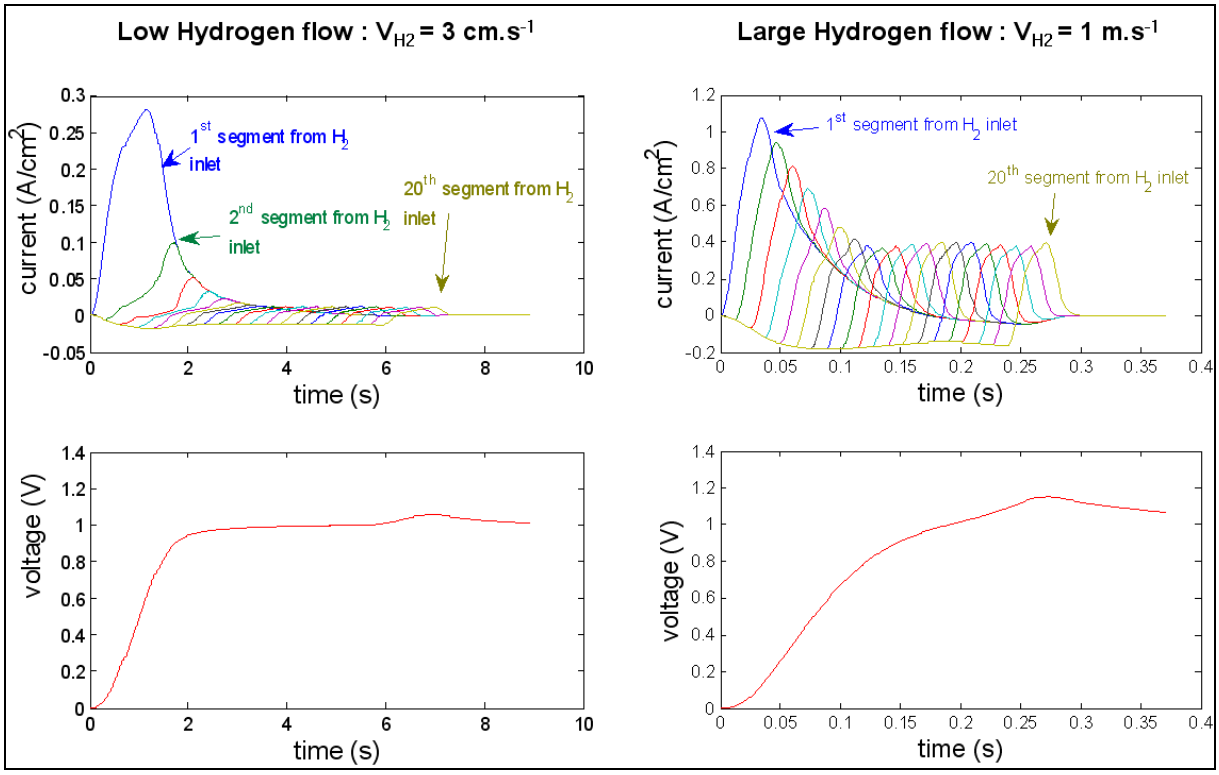

Figure 6: Numerical results obtained with E_0 = 1 V, R_m = 0.4 Ωcm^2, C_{dla} = C_{dlc} = 0.02 Fcm^{-2}, R_∞=1 Ωcm^2, R_{tc} =0.2 Ωcm^2 and R_{ta} = 0.05 Ωcm^2.

References

[1] Y. Shao, G. Yin, Y. Gao, Review: understanding and approaches for the durability issues of Pt-based catalysts for PEM fuel cell, J. Power Sources, 171 (2007) 558-566.

[2] S.D. Knights, K.M. Colbow, J. St-Pierre, D.P.Wilkinson, J. Power Sources, 127 (2004) 127

[3] P. Yu, M. Pemberton, P. Plasse, J. Power Sources 144 (2005) 11.

[4] T. Akita, A. Taniguchi, J. Maekawa, Z. Siroma, K. Tanaka, M. Kohyama, K. Yasuda, J. Power Sources 159 (2006) 461.

[5] H. Tang, Z. Qi, M.Ramani, J.F. Elter, PEM fuel cell cathode carbon corrosion due to the formation of air/fuel boundary at the anode, J. Power Sources, 158 (2006) 1306-1312.

[6] Q. Shen, M.Hou, D.Liang, Z.Zhou, X. Li, Z. Shao, B. Yi, Study on the processes of start-up and shut-down in proton exchange membrane fuel cells, J. Power Sources, 189 (2009), 1114-1119.

[7] J. Kim, J. Lee, Y. Tak, Relationship between carbon corrosion and positive electrode potential in a proton-exchange membrane fuel cell during start/stop operation, J. Power Sources, 192 (2009), 674-678.

[8] C. A. Reiser, L. Bregoli, T. W. Paterson, J. S. Yi, J. D. Yang, M.L. Perry, T.D. Jarvi, A reverse-current decay mechanism for fuel cells, Electrochemical and Solid-State Letters, 8 (6) A273-A276 (2005).

[9] J.P. Meyers, R. Darling, Model of carbon corrosion in PEM fuel cells, J. Electrochemical Society, 153 (8) A1432-A1442 (2006).

[10] N. Takeuchi; T.F. Fuller, Modeling and investigation of design factors and their impact on carbon corrosion of PEMFC electrodes, J. Electrochemical Society, 155 (7) B770-B775 (2008).

[11] Z. Siroma, N. Fujiwara, T. Ioroi, S. Yamazaki, H. Senoh, K. Yasuda, K. Tanimoto, Transient phenomena in a PEMFC during the start-up of gas feeding observed with a 97-fold segmented cell, J. Power Sources, 172 (2007), 155-162.

[12] G. Maranzana, O. Lottin, T. Colinart, S. Chupin, S. Didierjean, A multi-instrumented polymer exchange membrane fuel cell: Observation of the in-plane non-homogeneities, J. Power Sources, 180 (2008), 748-754.